#767

# On the Equivalence of Two Conceptual Models for Describing Ion Exchange During Transport Through an Aggregated Oxisol

P. Nkedi-Kizza,[1,2] J. W. Biggar,[1] H. M. Selim,[3] M. Th. van Genuchten,[4]
P. J. Wierenga,[5] J. M. Davidson,[6] and D. R. Nielsen[1]

Breakthrough curves (BTCs) of the cation $^{45}Ca^{2+}$, an anion $^{36}Cl^-$, and $^3H_2O$ were measured during miscible displacement through water-saturated soil columns packed with aggregates of an Oxisol. Two conceptual models were used to simulate the observed asymmetry and tailing in the BTCs caused by an apparent nonequilibrium situation in the porous medium. In both models the exchange process on one type of site was assumed to be instantaneous while the rate of isotopic exchange on another type of site was assumed to be either a diffusion-controlled process (model 1) or a first-order reversible kinetic process (model 2). Isotopic exchange in both models was described with a linear isotherm. It is shown that the two models are mathematically equivalent with respect to the derived BTCs.

## Introduction

Kinetic studies with the batch equilibration method have suggested that ion exchange is an instantaneous process [Hiss-ink, 1924; Borland and Reitemeier, 1950]. This should be expected since ion exchange is a physical stochiometric process with $\Delta H$ values of about 2 kcal mol$^{-1}$, resembling dipole-dipole interactions [Helfferich, 1962]. The interdiffusion of counter ions from the solution to the exchanger and vice versa, called ion exchange, is probably the main step that limits instantaneous equilibrium. This suggests that diffusion to and from the exchange sites, rather than the actual exchange reaction itself, determines the apparent exchange rate [Helfferich, 1962]. Because of relatively small particles normally used in batch ion-exchange kinetic studies, and because of vigorous shaking, diffusion often can be eliminated as a rate-limiting step [Boyd et al., 1947; Helfferich, 1962]. However, in a system with flowing water, and especially in aggregated soils, the ion-exchange rate can be limited by the rate at which the ions are transported by diffusion to the exchange sites. Several researchers [Smith, 1968; Nkedi-Kizza et al., 1982] have shown that even if the point reaction is instantaneous, the global or space kinetics can be influenced by such variables as fluid velocity (which is related to residence time) or aggregate size (which determines the diffusion path length).

Boyd et al. [1947] recognized two potential rate-limiting steps for ion-exchange kinetics: (1) intradiffusion of counter ions within the ion exchanger (particle diffusion) and (2) interdiffusion of counter ions in the adherent films (film diffusion). In practice, either step can be rate limiting, and for some cases the rate may be affected by both steps [Boyd et al., 1947; Hiester and Vermeulen, 1948; Lapidus and Amundson, 1952].

Various empirical equations resembling chemical kinetic rate laws have been used to describe the global kinetics of ion exchange [du Domaine et al., 1943; Thomas, 1944; Juda and Carron, 1948; Helfferich, 1962]. From a global (macroscopic) point of view, similar effects on chemical transport can be expected for certain rate laws that are based on diffusion mechanisms and for certain rate laws that are based on chemical kinetics [Hiester and Vermeulen, 1952; van Genuchten, 1981]. One kinetic rate equation that is applicable to heterogeneous exchange and macroscopically closely resembles diffusion-controlled exchange was proposed by Selim et al. [1976]. In this paper we shall demonstrate the mathematical equivalence of the physical nonequilibrium (diffusion) model of van Genuchten and Wierenga [1976] and the chemical nonequilibrium (kinetic) model of Selim et al. [1976]. The resulting simulations from the transport models will be applied to isotopic exchange of $^{45}Ca$ and $^{36}Cl$ during miscible displacement through an aggregated Oxisol.

## Theory

### Model 1: Diffusion-Controlled Rate Law

This model was first proposed for nonadsorbed solutes by Coats and Smith [1964] and later extended to adsorbed solutes by van Genuchten and Wierenga [1976]. In this model the liquid phase of the soil is partitioned into "mobile" (macroporosity) and "immobile" (microporosity) regions. Convective-diffusive transport is confined to the mobile water phase, while transfer of solutes into and out of the immobile (nonmoving) soil-water region is assumed to be diffusion controlled. The rate of solute transfer into the immobile regions is taken to be proportional to the difference in concentration between the two liquid regions. The governing transport equations for the mobile and immobile water phases are, respectively

$$\theta_m \frac{\partial c_m}{\partial t} + f\rho \frac{\partial s_m}{\partial t} + \theta_{im} \frac{\partial c_{im}}{\partial t} + (1-f)\rho \frac{\partial s_{im}}{\partial t}$$

$$= \theta_m D_m \frac{\partial^2 c_m}{\partial z^2} - \theta_m v_m \frac{\partial c_m}{\partial z} \quad (1)$$

$$\theta_{im} \frac{\partial c_{im}}{\partial t} + (1-f)\rho \frac{\partial s_{im}}{\partial t} = \alpha_1(c_m - c_{im}) \quad (2)$$

where $c$ and $s$ represent the concentrations associated with the liquid and solid phases of the soil, respectively, and where the subscripts $m$ and $im$ refer to the dynamic (mobile) and stag-

[1] Department of Land, Air and Water Resources, University of California, Davis.
[2] Now at Department of Soil Science, University of Florida, Gainesville.
[3] Department of Agronomy, Louisiana State University, Baton Rouge.
[4] U.S. Salinity Laboratory, USDA, Riverside, California.
[5] Department of Agronomy, New Mexico State University, Las Cruces.
[6] Department of Soil Science, University of Florida, Gainesville.

nant (immobile) fluid regions. The parameter $f$ represents the mass fraction of solid phase that is in direct contact with the mobile liquid phase. The remaining symbols in these and the following equations are defined in the notation list.

Isotopic exchange of $^{45}Ca$ and $^{36}Cl$ in both the dynamic and stagnant regions of the soil is assumed to be an instantaneous, linear, and reversible process. Therefore

$$s_m = K_D c_m \qquad s_{im} = K_D c_{im} \tag{3}$$

and total adsorption is

$$s = f s_m + (1 - f) s_{im} \tag{4}$$

The transport equations reduce to

$$(\theta_m + \rho f K_D) \frac{\partial c_m}{\partial t} + [\theta_{im} + (1 - f)\rho K_D] \frac{\partial c_{im}}{\partial t}$$
$$= \theta_m D_m \frac{\partial^2 c_m}{\partial z^2} - \theta_m v_m \frac{\partial c_m}{\partial z} \tag{5}$$

$$[\theta_{im} + (1 - f)\rho K_D] \frac{\partial c_{im}}{\partial t} = \alpha_1 (c_m - c_{im}) \tag{6}$$

The imposed initial and boundary conditions are

$$c_m(z, 0) = c_{im}(z, 0) = 0 \tag{7a}$$

$$-D_m \frac{\partial c_m}{\partial z} + v_m c_m\big|_{z=0} = v_m C_0 \qquad 0 < \tau \leq t_0 \tag{7b}$$
$$= 0 \qquad t \geq t_0$$

$$\frac{\partial c_m}{\partial z}(\infty, t) = \frac{\partial c_{im}}{\partial z}(\infty, t) = 0 \tag{7c}$$

Let us introduce the following dimensionless variables:

$$c_1 = c_m/C_0 \qquad c_2 = c_{im}/C_0 \tag{8}$$

$$T = \frac{vt}{L} = \frac{v_m \phi_m t}{L} \qquad \phi_m = \frac{\theta_m}{\theta} \tag{9}$$

$$x = z/L \tag{10}$$

$$P = \frac{v_m L}{D_m} \tag{11}$$

$$R = 1 + \frac{\rho K_D}{\theta} \tag{12}$$

$$\beta = \frac{\theta_m + f\rho K_D}{\theta + \rho K_D} = \frac{\phi_m R_m}{R} \qquad R_m = 1 + \frac{f\rho K_D}{\theta_m} \tag{13}$$

$$\omega = \frac{\alpha_1 L}{q} \qquad q = \theta_m v_m \tag{14}$$

Substitution of these variables into (5) and (6) gives the final form of the transport model:

$$\beta R \frac{\partial c_1}{\partial T} + (1 - \beta) R \frac{\partial c_2}{\partial T} = \frac{1}{P} \frac{\partial^2 c_1}{\partial x^2} - \frac{\partial c_1}{\partial x} \tag{15}$$

$$(1 - \beta) R \frac{\partial c_2}{\partial T} = \omega(c_1 - c_2) \tag{16}$$

Similarly, the initial and boundary conditions become

$$c_1(x, 0) = c_2(x, 0) = 0 \tag{17a}$$

$$-\frac{1}{P} \frac{\partial c_1}{\partial x} + c_1\big|_{x=0} = 1 \qquad 0 < T \leq T_0 \tag{17b}$$
$$= 0 \qquad T > T_0$$

$$\frac{\partial c_1}{\partial x}(\infty, T) = \frac{\partial c_2}{\partial x}(\infty, T) = 0 \tag{17c}$$

The analytical solution of (15), (16), and (17) is given elsewhere [van Genuchten and Wierenga, 1976].

*Model 2: Surface Reaction Rate Law*

Combined equilibrium and kinetic models to describe solute adsorption on heterogeneous solid surfaces were proposed independently by *Selim et al.* [1976] and by *Cameron and Klute* [1977]. This type of model was used later also by *Rao et al.* [1979] for pesticide adsorption and by *De Camargo et al.* [1979] and *Hoffman and Rolston* [1980] for phosphorus adsorption. In this model, two types of adsorption sites are hypothesized: type 1 sites that achieve instantaneous equilibrium and type 2 sites with time-dependent kinetic adsorption. At equilibrium, adsorption on both sites is described by linear equations:

$$s_1 = K_1 c = F K_D c \tag{18}$$

$$s_2 = K_2 c = (1 - F) K_D c \tag{19}$$

where the subscripts 1 and 2 now refer to type 1 (equilibrium) and type 2 (kinetic) sites respectively, and where $F$ is the fraction of all sites that are type 1. Total adsorption at equilibrium is simply

$$s = s_1 + s_2 \tag{20}$$

Because type 1 sites are always at equilibrium, it follows from (18) that

$$\frac{\partial s_1}{\partial t} = F K_D \frac{\partial c}{\partial t} \tag{21}$$

The adsorption rate for the type 2 kinetic nonequilibrium sites is given by a linear and reversible first-order equation of the form

$$\frac{\partial s_2}{\partial t} = \alpha_2 [(1 - F) K_D c - s_2] \tag{22}$$

where the model-specific parameter $\alpha_2$ now represents a first-order kinetic rate coefficient. The governing transport equations for model 2 are

$$\left[ 1 + \frac{F\rho K_D}{\theta} \right] \frac{\partial c}{\partial t} + \frac{\rho}{\theta} \frac{\partial s_2}{\partial t} = D \frac{\partial^2 c}{\partial z^2} - v \frac{\partial c}{\partial z} \tag{23}$$

$$\frac{\partial s_2}{\partial t} = \alpha_2 [(1 - F) K_D c - s_2] \tag{24}$$

The initial and boundary conditions for model 2 are

$$c(z, 0) = s_2(z, 0) = 0 \tag{25a}$$

$$-D \frac{\partial c}{\partial z} + vc\bigg|_{z=0} = vC_0 \qquad 0 < t \leq t_0 \tag{25b}$$
$$= 0 \qquad t > t_0$$

$$\frac{\partial c}{\partial z}(\infty, t) = \frac{\partial s_2}{\partial z}(\infty, t) = 0 \tag{25c}$$

The following dimensionless variables are introduced for model 2:

$$c_1 = \frac{c}{C_0} \qquad c_2 = \frac{s_2}{(1 - F) K_D C_0} \tag{26}$$

TABLE 1. Soil Column Data for Various Displacements Through the Ione Oxisol

| Column No. | Experiment No. | Aggregate Diameter, mm | Concentration $N$ | pH | Bulk Density $\rho$, g cm$^{-3}$ | Water Content $\theta$, cm$^3$ cm$^{-3}$ | Flux $q$, cm h$^{-1}$ | Pulse $T_1$ Pore Volumes | Tracer |
|---|---|---|---|---|---|---|---|---|---|
| 1 | 1 | 0.5–1 | 0.1 | 4 | 1.18 | 0.52 | 0.94 | 0.32 | $^{36}$Cl |
| 1 | 2 | 0.5–1 | 0.01 | 4 | 1.18 | 0.52 | 0.94 | 0.44 | $^{36}$Cl |
| 1 | 3 | 0.5–1 | 0.001 | 4 | 1.18 | 0.52 | 0.89 | 0.45 | $^{36}$Cl |
| 2 | 4 | 0.5–1 | 0.01 | 4 | 1.09 | 0.56 | 0.25 | 0.31 | $^{36}$Cl |
| 3 | 5 | 0.5–1 | 0.1 | 7 | 1.24 | 0.58 | 3.41 | 0.50 | $^{45}$Ca |
| 3 | 6 | 0.5–1 | 0.1 | 7 | 1.24 | 0.58 | 0.25 | 0.38 | $^{45}$Ca |
| 4 | 7 | 2–4.7 | 0.1 | 7 | 1.25 | 0.58 | 3.20 | 0.39 | $^{45}$Ca |
| 4 | 8 | 2–4.7 | 0.1 | 7 | 1.25 | 0.58 | 0.26 | 0.35 | $^{45}$Ca |

$$T = \frac{vt}{L} \qquad x = \frac{z}{L} \tag{27}$$

$$P = \frac{vL}{D} \tag{28}$$

$$R = 1 + \frac{\rho K_D}{\theta} \qquad R_m = 1 + \frac{F\rho K_D}{\theta} \tag{29}$$

$$\beta = \frac{\theta + F\rho K_D}{\theta + \rho K_D} = \frac{R_m}{R} \tag{30}$$

$$\omega = \frac{\alpha_2(1 - \beta)RL}{v} \tag{31}$$

Note that some of these variables ($T$, $x$, $R$) are the same as for model 1. Substitution of the dimensionless variables into (23) and (24) leads to the same dimensionless transport equations as for model 1 (equations (15) and (16)). Because the dimensionless boundary conditions are also the same, it follows immediately that the dimensionless analytical solutions for models 1 and 2 are identical.

## MATERIALS AND METHODS

### Miscible Displacement Studies

Breakthrough curves (BTCs) of $^{45}$Ca, $^{36}$Cl, and $^3$H$_2$O, applied together as a pulse to soil columns packed with an aggregated Oxisol, were measured under water-saturated, steady-flow conditions. Physical and chemical properties of the Ione Oxisol have been given elsewhere [Singer and Nkedi-Kizza, 1980; Nkedi-Kizza, 1979]. In summary, the soil is strongly aggregated, has a pH of 3.7, a cation exchange capacity (CEC) of 2 meq/100 g soil, an Fe$_2$O$_3$ content of 6.5%, a zero point of charge at pH 3.6, and has kaolinite as the predominant clay mineral. The soil was adjusted to a pH of either 4 or 7 and separated into aggregate fractions of 0.5–1.0 and 2.0–4.0 mm in diameter. Each aggregate fraction was first saturated with 0.1 $N$ CaCl$_2$ and then packed separately into Plexiglas cylinders, 45 cm$^2$ in cross-sectional area and 5 cm long. Details of the procedure used to adjust the soil pH, the pH of the applied solution concentrations, the simultaneous determination of the three isotopes in one sample, and the miscible displacement experiments themselves are given by Nkedi-Kizza [1979]. The BTCs were measured using 0.1, 0.01, and 0.001 $N$ CaCl$_2$ solutions that were adjusted to the final pH of the soil. The pulse solutions of CaCl$_2$ were spiked with $^{45}$Ca, $^{36}$Cl, and $^3$H$_2$O, each giving about 5 nCi/ml. Table 1 summarizes column data for the various displacement experiments. The displacements through the same column were run in the same order as presented in the table. For example, for

column 1 the experiments were run from experiment 1 through 3.

### Model Parameter Estimation

The analytical solution of (15)–(17) contains the four independent parameters $P$, $R$, $\beta$, and $\omega$. Experimental methods currently are unavailable to measure parameters $\beta$ and $\omega$ independently. The initial estimates of $P$, $\beta$, and $\omega$ for $^{36}$Cl or $^{45}$Ca breakthrough curves were obtained by curve fitting the analytical solution to the experimental effluent curves of $^3$H$_2$O. The nonlinear curve-fitting program of van Genuchten [1981] was used for this purpose and for estimating $R$, $\beta$, and $\omega$ of $^{36}$Cl$^-$ and $^{45}$Ca$^{2+}$ effluent curves. For BTCs obtained from the same experiment for $^3$H$_2$O, $^{36}$Cl$^-$, and $^{45}$Ca$^{2+}$, the estimated parameter $P$ from $^3$H$_2$O effluent curves was not optimized during the estimation of the remaining parameters ($R$, $\beta$, and $\omega$) for $^{36}$Cl$^-$ or $^{45}$Ca$^{2+}$. Thus the task was reduced to estimating three parameters ($R$, $\beta$, and $\omega$).

## RESULTS AND DISCUSSIONS

### Breakthrough Curves

Figures 1–8 show measured and calculated BTC for either $^{36}$Cl$^-$ or $^{45}$Ca$^{2+}$. The measured BTC for each experiment is represented by solid circles, while the simulated BTC is shown as a solid line. Table 2 summarizes the dimensionless parameter values obtained using model simulations for each experiment. For Figures 1–3, BTCs were obtained from the same column, except that the carrier concentration was reduced from 0.1 $N$ to 0.001 $N$ CaCl$_2$. The retardation factor for all three displacements is greater than 1 for $^{36}$Cl$^-$, implying sorp-
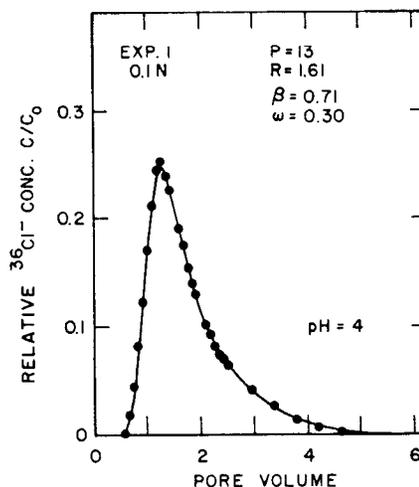


Fig. 1. Observed (solid circles) and fitted (solid lines) breakthrough curves for experiment 1: $^{36}$Cl in 0.1 $N$ CaCl$_2$.

TABLE 2. Fitted Values for the Dimensionless Parameters $P$, $R$, $\beta$, and $\omega$

| Column No. | Experiment No. | $P$ | $R$ | $\beta$ | $\omega$ | Tracer |
|---|---|---|---|---|---|---|
| 1 | 1 | 13 | $1.61 \pm 0.04$ | $0.71 \pm 0.02$ | $0.30 \pm 0.10$ | $^{36}Cl$ |
| 1 | 2 | 13 | $1.89 \pm 0.06$ | $0.73 \pm 0.03$ | $0.69 \pm 0.19$ | $^{36}Cl$ |
| 1 | 3 | 13 | $4.46 \pm 0.08$ | $0.74 \pm 0.10$ | $0.59 \pm 0.10$ | $^{36}Cl$ |
| 2 | 4 | 13 | $1.89 \pm 0.34$ | $0.88 \pm 0.12$ | $0.16 \pm 0.12$ | $^{36}Cl$ |
| 3 | 5 | 8 | $2.88 \pm 0.07$ | $0.67 \pm 0.03$ | $1.74 \pm 0.34$ | $^{45}Ca$ |
| 3 | 6 | 8 | $2.39 \pm 0.19$ | $0.67 \pm 0.03$ | $1.55 \pm 0.34$ | $^{45}Ca$ |
| 4 | 7 | 4 | $1.83 \pm 0.11$ | $0.57 \pm 0.03$ | $0.18 \pm 0.02$ | $^{45}Ca$ |
| 4 | 8 | 4 | $1.60 \pm 0.20$ | $0.57 \pm 0.03$ | $0.59 \pm 0.13$ | $^{45}Ca$ |

Fitted values include the 95% confidence interval.

tion at $pH = 4$. It should be pointed out that the method of van Raij and Peech [1972] used to determine the zero point of charge (ZPC) of the Ione Oxisol [Nkedi-Kizza, 1979] tends to give lower ZPC (lower $pH$) than that obtained by anion retention. Espinoza et al. [1975] found ZPC resulting from nitrate retention to be significantly higher than that obtained by the method of van Raij and Peech [1972]. Thus it is not surprising that $^{36}Cl^-$ is sorbed by the Ione Oxisol at $pH = 4.0$. From the $R$ values in Table 2, it is clear that the sorption of trace amounts of $^{36}Cl^-$ in the system increases with a decrease in solution concentration of the carrier solution (Figures 1–3). A similar trend of data was obtained by Persaud et al. [1983] for sorption and leaching of $Na^+$ and $Li^+$ in decreasing concentrations of $Ca(NO_3)_2$. During the model simulations the Peclet number value of 13 initially obtained for the $^3H_2O$ effluent curve for experiment 1, was used for BTCs in Figures 1–3. The only parameters optimized were $R$, $\beta$, and $\omega$.

In Figure 4 the BTC of $^{36}Cl$ in a column packed with aggregate of the same size as for column 1 is presented. The experiment was run at a flux 4 times less with $0.01$ $N$ $CaCl_2$ as carrier solution. Thus the Peclet number of 13 was fixed for this simulation, since Nkedi-Kizza et al. [1983] found a linear relationship between the dispersion coefficient $D_m$ and velocity $v_m$. The $R$ and $\beta$ values obtained for this experiment are not significantly different from those of experiment 2, which was run under similar conditions except for the flux. Thus $R$ and $\beta$ values obtained from experiment 2 could have been used to describe the BTC for experiment 4 (Table 2).

Figures 5 and 6 show BTCs of $^{45}Ca$ for the same column,

but experiment 5 was run at a flux 14 times greater than that of experiment 6. Again as for $^{36}Cl$ effluent curves, the $P$ value of 8 for both experiments was obtained from the $^3H_2O$ effluent curve simulation. Thus only the parameters $R$, $\beta$, and $\omega$ were optimized for experiment 5. Since Nkedi-Kizza et al. [1983] pointed out that the best estimate of $\beta$ is from high flow velocity experiments, the $\beta$ value from experiment 5 was used to simulate BTC for experiment 6. Thus the parameters $R$ and $\omega$ were optimized to simulate the BTC for experiment 6. It should be pointed out that the $R$ value for experiment 5 is higher than that for experiment 6. Since $K_D$ is not a function of velocity, the possible explanation is that the $pH$ for experiment 5 might have been somewhat higher than that of experiment 6. Since CEC is a function of $pH$ in this soil, the higher $pH$ would increase $K_D$ and thus $R$.

In Figures 7 and 8 the BTCs for $^{45}Ca$ are presented for experiments run through the soil column packed with aggregates of 2–4.7 mm in diameter. Experiment 7 was run at a flux 12 times larger than that of experiment 8. The $P$ value of 4 (Table 2) was obtained from $^3H_2O$ simulations of effluent curves for both experiments. Thus initially, the parameters $R$, $\beta$, and $\omega$ were optimized for experiment 7 and the $\beta$ value obtained was used in simulating the BTC for experiment 8. Thus only the parameters $R$ and $\omega$ were optimized for experiment 8. From Table 2 the $R$ values for experiments 7 and 8 are not significantly different; thus both BTC could not be simulated using the same values of the parameters $P$, $R$, and $\beta$.

The most inconsistent parameter in all these simulations is $\omega$. This parameter seems to be influenced by aggregate size,
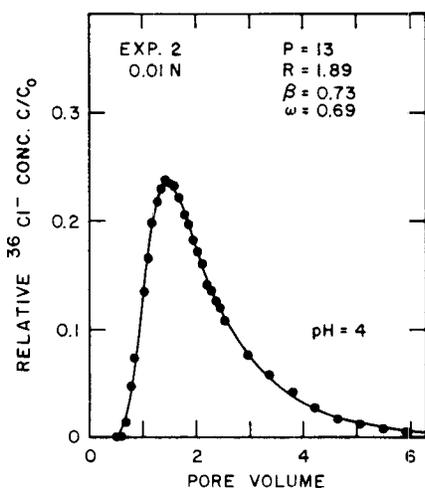


Fig. 2. Observed (solid circles) and fitted (solid lines) breakthrough curves for experiment 2: $^{36}Cl$ in $0.01$ $N$ $CaCl_2$.
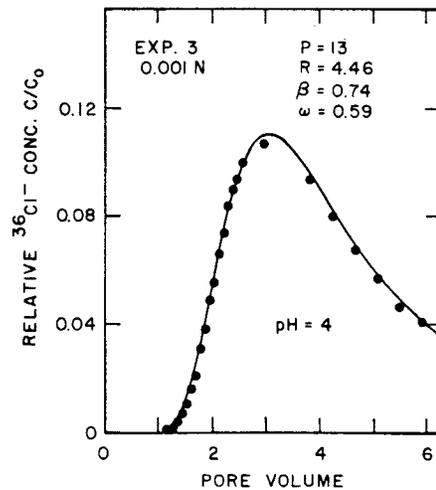


Fig. 3. Observed (solid circles) and fitted (solid lines) breakthrough curves for experiment 3: $^{36}Cl$ in $0.001$ $N$ $CaCl_2$.

Fig. 4. Observed (solid circles) and fitted (solid lines) break-through curves for experiment 4. Conditions are similar to experiment 3 but flux is 4 times slower.
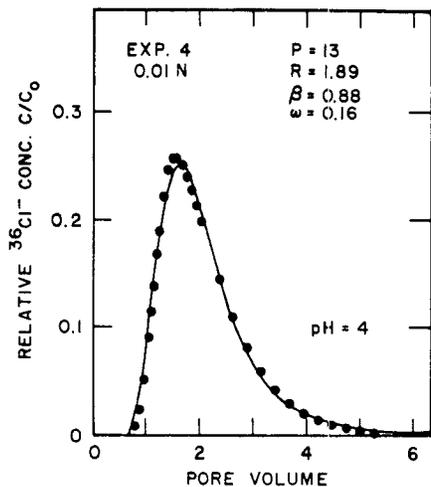


Fig. 6. Observed (solid circles) and fitted (solid lines) break-through curves for experiment 6. Conditions are similar to experiment 5 but flux is 14 times slower.

flux, and concentration of carrier solution. *Rao et al.* [1980] have pointed out that for a given ionic species, $\omega$ is not a constant but a function of aggregate size, flux, and mobile water. In this study we find $\omega$ to be a function of solution concentration also. It seems more work is needed to characterize $\omega$ with respect to the nature of porous medium and experimental conditions imposed on the system.

### Estimates for the Original Model Parameters

Table 2 gives the fitted values of the four dimensionless parameters $(P, R, \beta, \text{and } \omega)$ in the general transport model. Of these, the column Peclet number $P$ can be viewed approximately as the ratio of the residence times for diffusive $(L^2/D_m$ or $L^2/D)$ and convective transport $(L/v_m$ or $L/v)$. From Table 2 it is apparent that the same $P$ value can be used to simulate effluent curves run through the same column even if flux and solution concentration are varied. The data presented with respect to $P$ confirm earlier data presented by *Nkedi-Kizza et al.* [1983] for $^3H_2O$ and $^{36}Cl$ leached simultaneously through the same column.

The retardation factor $R$ reflects the effects of adsorption during transport through the Ione soil. The parameter $\beta$ de-
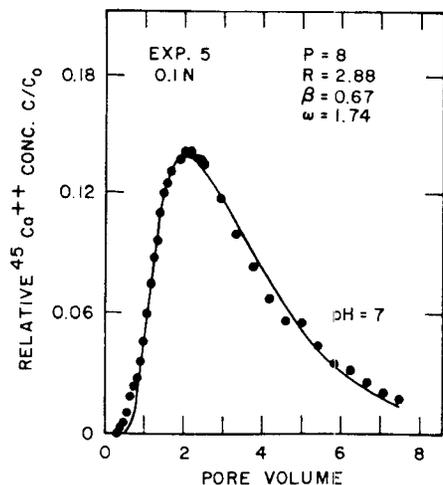
scribes the maximum degree of nonequilibrium in the system, either in a physical (model 1) or chemical-kinetic sense (model 2). Finally, the mass transfer coefficient $\omega$ describes the rate at which equilibrium is obtained from the initial nonequilibrium situation; the larger $\omega$ is, the sooner equilibrium is obtained.

Once the dimensionless parameters have been quantified, estimates for the original parameters in the two conceptual models can be derived by appropriately inverting the dimensionless quantities. Table 3 gives the inverted expressions that can be used as a guide for deriving estimates for the original parameters. Use of this table is straightforward, except with respect to the inverted expressions for the dimensionless parameter $\beta$ in model 1. This parameter contains the unknown quantities $\phi_m$ (fraction of water considered to be mobile) and $f$ (fraction of adsorption sites located in the dynamic region). For example, from Table 2 we have

$$\phi_m = \beta R - f(R - 1) \qquad (32)$$

This equation shows that, first, an estimate of $f$ is needed before $\phi_m$ can be calculated from $\beta$ or, conversely, that an estimate for $\phi_m$ is needed before $f$ can be calculated.

At least four alternative procedures can be followed to



Fig. 5. Observed (solid circles) and fitted (solid lines) break-through curves for experiment 5: $^{45}Ca$ in 0.1 $N$ $CaCl_2$ and aggregates of 0.5–1.0 mm in diameter.



Fig. 7. Observed (solid circles) and fitted (solid lines) break-through curves for experiment 7: $^{45}Ca$ in 0.1 $N$ $CaCl_2$ and aggregates of 2–4.7 mm in diameter.
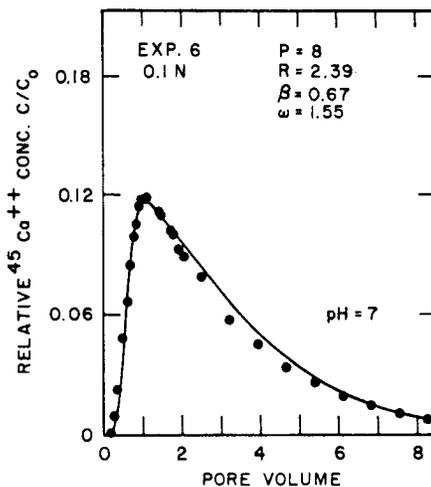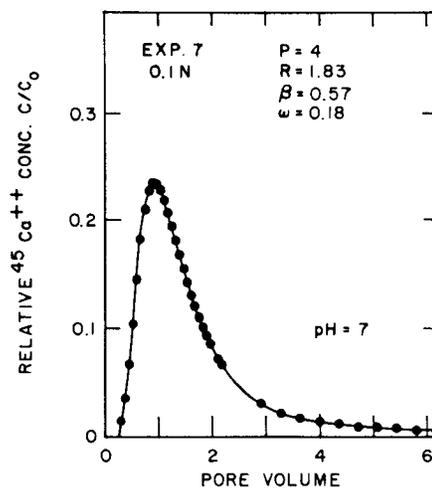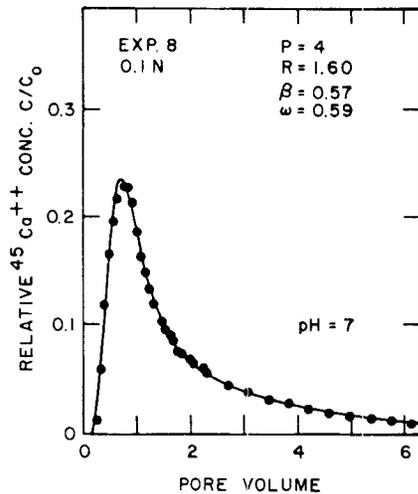
Fig. 8. Observed (solid circles) and fitted (solid lines) break-through curves for experiment 8. Conditions are similar to experiment 7 but flux is 12 times slower.

obtain estimates for $\phi_m$ and $f$. One method would be to carry out displacement experiments on the same soil column and at the same flow velocity but with a tracer that does not interact or only weakly interacts with the solid phase [Gaudet et al., 1977; De Smedt, 1979]. This approach yields an estimate for $\phi_m$ that should be characteristic for the prevailing aggregate size and flow velocity. A second approach would be to obtain BTCs from the same soil column using two chemicals that are adsorbed by similar sorption sites but at different strengths. Assuming $\phi_m$ and $f$ to be the same for the two chemical-soil combinations, the procedure would lead to two simultaneous equations in two unknowns, the solution of which yields estimates for $\phi_m$ and $f$ [van Genuchten and Clearly, 1979].

As a third approach, one could simply assume that $f$ equals zero, thereby assuming that tracer adsorption takes place only in the stagnant region of the soil, i.e., inside the aggregates [Bolt, 1979; Nkedi-Kizza et al., 1982]. This assumption appears realistic for those soils in which the interior surface area of the aggregates is much larger than the exterior surface area. The assumption that $f = 0$, however, is less realistic for soils that are only weakly aggregated. In fact, for the limiting case when all soil water becomes mobile, all adsorption sites would become completely inaccessible for the chemical in the displacing fluid.

A fourth approach, and the one followed here, assumes that $f$ and $\phi_m$ are numerically equal and that they are similar functions of the physical makeup of the soil (mainly aggregate size). When $\phi_m$ is small and large quantities of relatively immobile water are stored inside the aggregates, one may assume that only a few of the adsorption sites are readily accessible for the displacing chemical ($f$ is small). On the other hand, when all soil water becomes mobile ($\phi_m = 1$), one may assume that most of the adsorption sites are also readily accessible

($f = 1$). In that case, model 1 would then reduce to the classical convective-diffusive transport model [Lindstrom et al., 1967]. A possible situation that may not conform to this description would be the leaching process through soils with extremely dense aggregates that have large internal surface areas but, at the same time, contain only little intraaggregate water [Bolt, 1979]. The assumption that $f$ equals $\phi_m$ leads to the simple equation

$$\phi_m = f = \beta \qquad (33)$$

Using (33), it is now possible to obtain estimates for the original parameters in model 1. The various estimates are given in Table 4. Note that the $K_D$ values for the two models are the same ($R$ is the same). The dependency of the sorption coefficient $K_D$ (for isotopic exchange) on solution concentration is evident from Table 2 while comparing experiments 1–3 for $^{36}Cl$. The dispersion increases with velocity, and the fraction of "sites" at equilibrium decreases with an increase in aggregate size. The mass transfer coefficient $\alpha_1$ or the first-order kinetic coefficient $\alpha_2$ seems to become larger with an increase in flux. Since the residence time of a solute in a porous medium is a measure of the time available for diffusive mass exchange between the stagnant and mobile water regions in the porous medium, $\alpha$ should decrease with a decrease in flux as indicated in Table 3. This is a result of an increase in time over which $\alpha$ is calculated [Rao et al., 1980].

## Mathematical Equivalence of Models 1 and 2

The theoretical sections show that the two conceptually different models 1 and 2 can be put into the same dimensionless form. In this study we have measured only breakthrough curves. The dimensionless dependent variable $c_1(x, T)$, evaluated at $x = 1$, describes in mathematical terms these breakthrough curves for both models. Therefore the models are mathematically equivalent with respect to their BTCs. However, the two models are not equivalent with respect to measurements inside the column. For example, the dependent dimensionless concentration variable $c_2$ for model 1 is associated with a certain fraction of the liquid phase, while for model 2, it refers to a fraction of the solid phase. Furthermore, the variable $c_1$ itself is associated with different parts of the porous medium inside the column: mobile liquid in model 1 and total liquid in model 2. It follows therefore that only careful (microscopic) determinations of certain parameters (in situ) inside the column ($c$, $c_1$, $s_1$) could be used to verify the conceptual basis of the two models. However, such a verification cannot be made by using only measured effluent curves.

From this it follows that the measured BTCs in this study cannot be used to differentiate between the exact physical and chemical aspects of the apparent nonequilibrium situation inside the column. The question immediately arises whether such a differentiation between physical and chemical aspects is possible, important, and really needed. Model 1 is con-

TABLE 3. Expressions for the Original Parameters in Models 1 and 2 in Terms of the Dimensionless Parameters $P$, $R$, $\beta$, and $\omega$

|         | $P$ | $R$ | $\beta$ | $\omega$ |
|---------|-----|-----|---------|----------|
| Model 1 | $D_m = (qL)/(\theta_m P)$ | $K_D = [\theta(R-1)]/\rho$ | $\phi_m = \beta R + f(R-1)$ <br> $f = (\beta R - \phi_m)/(R-1)$ | $\alpha_1 = (\omega q)/L$ |
| Model 2 | $D = (vL)/P$ | $K_D = [\theta(R-1)]/\rho$ | $F = (\beta R - 1)/(R-1)$ | $\alpha_2 = (\omega v)/[(1-\beta)RL]$ |

TABLE 4. Derived Values for the Original Parameters in Models 1 and 2

| Experiment No. | Model 1 | | | | Model 2 | | | | Tracer |
|---|---|---|---|---|---|---|---|---|---|
| | $D_m$, cm$^2$ h$^{-1}$ | $K_D$, cm$^3$ g$^{-1}$ | $f$ | $\alpha_1$, h$^{-1}$ | $D$, cm$^2$ h$^{-1}$ | $K_D$, cm$^3$ g$^{-1}$ | $F$ | $\alpha_2$, h$^{-1}$ | |
| 1 | $0.98 \pm 0.02$ | $0.26 \pm 0.01$ | $0.71 \pm 0.02$ | $0.06 \pm 0.02$ | 0.70 | $0.26 \pm 0.01$ | $0.23 \pm 0.08$ | 0.25 | $^{36}$Cl |
| 2 | $0.95 \pm 0.04$ | $0.39 \pm 0.02$ | $0.73 \pm 0.03$ | $0.13 \pm 0.04$ | 0.70 | $0.39 \pm 0.02$ | $0.43 \pm 0.10$ | 0.49 | $^{36}$Cl |
| 3 | $0.94 \pm 0.14$ | $1.52 \pm 0.03$ | $0.74 \pm 0.10$ | $0.11 \pm 0.02$ | 0.66 | $1.52 \pm 0.03$ | $0.66 \pm 0.13$ | 0.17 | $^{36}$Cl |
| 4 | $0.20 \pm 0.01$ | $0.46 \pm 0.10$ | $0.88 \pm 0.12$ | $0.01 \pm 0.01$ | 0.17 | $0.46 \pm 0.10$ | $0.75 \pm 0.42$ | 0.06 | $^{36}$Cl |
| 5 | $5.48 \pm 0.34$ | $0.88 \pm 0.03$ | $0.67 \pm 0.03$ | $1.19 \pm 0.24$ | 3.67 | $0.88 \pm 0.03$ | $0.49 \pm 0.05$ | 2.15 | $^{45}$Ca |
| 6 | $0.40 \pm 0.02$ | $0.65 \pm 0.09$ | $0.67 \pm 0.03$ | $0.08 \pm 0.02$ | 0.27 | $0.65 \pm 0.09$ | $0.43 \pm 0.10$ | 0.17 | $^{45}$Ca |
| 7 | $12.10 \pm 0.67$ | $0.39 \pm 0.06$ | $0.57 \pm 0.03$ | $0.12 \pm 0.02$ | 6.90 | $0.39 \pm 0.06$ | $0.05 \pm 0.00$ | 0.25 | $^{45}$Ca |
| 8 | $0.98 \pm 0.02$ | $0.27 \pm 0.08$ | $0.57 \pm 0.03$ | $0.03 \pm 0.01$ | 0.56 | $0.27 \pm 0.08$ | $0.03 \pm 0.00$ | 0.08 | $^{45}$Ca |

Derived values include the 95% confidence interval where desirable.

ceptually pleasing since it has an equivalent formulation for nonadsorbing systems [*Gaudet et al.*, 1977; *Coats and Smith*, 1964]. On the other hand, adsorption in this model is described with the assumption that the solid phase is homogeneous and hence that adsorption on all sites occurs with the same strength and at the same (equilbrium) rate. This assumption may not be realistic for usually heterogeneous soil systems. It appears more likely that the mechanisms of both models are present simultaneously in many soil systems. Thus the macroscopically oriented and semiempirical dimensionless transport model can be used without having to delineate the exact physical and chemical processes that operate in the system in a microscopic fashion. However, it should not be alarming to see that both models can be used to predict isotopic exchange during transport in an aggregated porous medium. We may emphasize once more that isotopic exchange is instantaneous and that both models are empirical in nature with regard to describing ionic diffusion to inaccessible sites in the system. Rigorously, diffusion of ionic species to inaccessible sites or regions in the porous medium should have been described by Fick's second law of diffusion, if the shape and sizes of aggregates were known exactly.

## SUMMARY AND CONCLUSIONS

This paper evaluated two conceptual models that describe isotopic exchange of $^{36}$Cl or $^{45}$Ca during transport through water-saturated aggregated soil columns. In both models, exchange on one type of sorption sites was assumed to be instantaneous, while the rate of exchange on another type of sites was assumed to be either a diffusion-controlled process (model 1) or a first-order reversible kinetic process (model 2). At equilibrium, isotopic exchange in both models was described with a linear reversible isotherm. By introducing appropriate dimensionless variables, both models could be put into exactly the same dimensionless form. The resulting dimensionless transport model contains two dependent variables ($c_1$ and $c_2$) and four independent parameters ($P$, $R$, $\beta$, and $\omega$).

Because the effluent curves in both models could be described by the same dependent variable ($c_1$), it follows that the two models are equivalent with respect to their breakthrough curves. Therefore both models were equally successful in describing the measured BTCs. However, the two dependent variables define conceptually different quantities in the two models. For example, $c_2$ in model 1 describes the average solution concentration of the immobile liquid zone, while $c_2$ in model 2 defines the adsorbed concentration associated with type 2 (kinetic) nonequilibrium sites. This shows that micro-

scopic measurements inside the column must be carried out to verify the conceptual basis of the two models.

In most cases the parameters $R$, $\beta$, and $\omega$ were estimated by curve fitting them to measured BTCs. The parameter $P$ was obtained from $^3$H$_2$O effluent curves and was therefore not optimized during model simulations and was found to be dependent only on physical characteristics of the porous medium (mainly aggregate size). The retardation factor $R$, which was defined similarly for the two models, depended mainly on pH and total electrolyte concentration of the feed solution. The parameter $\omega$ was found to be a function of both the physical (aggregate size, flow velocity) and chemical characteristics (e.g., total solute concentration) of the system, and the parameter $\beta$ was a function of aggregate size.

It is suggested that the difference between diffusion-controlled adsorption (model 1) and two-site kinetic adsorption (model 2) is of little practical importance when describing ion exchange during transport through aggregated sorbing media. Both models generate macroscopically the same total concentration distribution ($c_i + s_i$) in the system.

## NOTATION

$c$    solution concentration, nCi/cm$^3$ (model 2).

$C_0$    input concentration, nCI/cm$^3$.

$c_1$    dimensionless solution concentration of "mobile" liquid phase (model 1) or of total liquid phase (model 2).

$c_2$    dimensionless solution concentration of "immobile" liquid phase (model 1) or adsorbed concentration for type 2 kinetic sites (model 2).

$c_{im}$    average concentration of immobile liquid phase, nCi/cm$^3$.

$c_m$    average concentration of mobile liquid phase, nCi/cm$^3$.

$D$    apparent diffusion coefficient of total liquid phase, cm$^2$/h (model 2).

$D_m$    apparent diffusion coefficient of mobile liquid phase, cm$^2$/h (model 1).

$f$    mass fraction of adsorption sites in dynamic region (model 1).

$F$    fraction of adsorption sites in equilibrium with solution concentration (model 2).

$K_1$, $K_2$    distribution coefficients for type 1 (equilibrium) and type 2 (kinetic) sites, cm$^3$/g (model 2).

$K_D$    distribution coefficient for linear adsorption, cm$^3$/g.

$L$    column length, cm.

$P$    column Peclet number.

$q$    volumetric flux density, cm/h.

$R$    retardation factor.

$R_m$    retardation factor for dynamic region (model 1) or type 1 equilibrium sites (model 2).

$s$    total adsorbed concentration, nCi/g.

$s_1, s_2$    adsorbed concentrations associated with type 1 (equilibrium) and type 2 (kinetic) sites, nCi/g (model 2).

$s_{im}, s_m$    adsorbed concentrations in the dynamic and stagnant regions of the soil, respectively, nCi/g (model 1).

$t$    time, hours.

$t_1$    time of applied concentration pulse, hours.

$T$    pore volume.

$T_0$    dimensionless pulse time.

$v$    average pore-water velocity, cm/h.

$v_m$    average pore-water velocity in mobile liquid region, cm/h (model 2).

$x$    dimensionless distance.

$z$    distance, cm.

$\alpha_1^{\cdot}$    first-order mass transfer coefficient, per hour (model 1).

$\alpha_2$    first-order kinetic rate coefficient, per hour (model 2).

$\beta$    dimensionless partition coefficient.

$\theta$    volumetric water content.

$\theta_m$    volumetric water content in mobile region.

$\rho$    bulk density, g/cm$^3$.

$\phi_m$    fraction of liquid phase that is considered to be mobile (model 1).

$\omega$    dimensionless mass transfer coefficient.

## REFERENCES

Bolt, G. H., Movement of solutes in soil: Principles of adsorption/exchange chromatography, In *Soil Chemistry*, vol. B, *Physico-Chemical Models*, edited by, G. H. Bolt, pp. 285–348, Elsevier, New York, 1979.

Borland, J. W., and R. F. Reitemeier, Kinetic exchange studies on clays with radioactive calcium, *Soil Sci.*, 69, 251–259, 1950.

Boyd, G. E., A. W. Adamson, and L. S. Myers, The exchange adsorption of ions from aqueous solutions by organic zeolites, 2, Kinetics, *J. Am. Chem. Soc.*, 69, 2836–2848, 1947.

Cameron, D. A., and A. Klute, Convective-dispersive solute transport with a combined equilibrium and kinetic adsorption model, *Water Resour. Res.*, 13, 197–199, 1977.

Coats, K. H., and B. D. Smith, Dead-end pore volume and dispersion in porous media, *Soc. Pet. Eng. J.*, 4, 73-84, 1964.

De Camargo, O. A., J. W. Biggar, and D. R. Nielsen, Transport of inorganic phosphorus in an Alfisol, *Soil Sci. Soc. Am. J.*, 43, 884–890, 1979.

De Smedt, F., Theoretical and experimental study of solute movement through porous media with mobile and immobile water, Ph.D. dissertation, Fac. der Toegepaste Wetensch., Dienst Hydrol., Vrije Univ., Brussels, 1979.

du Domaine, J., R. L. Swain, and O. A. Hougen, Cation-exchange water softening rates, *Ind. Eng. Chem.*, 35, 546–553, 1943.

Espinoza, W., R. G. Gast, and R. S. Adams, Charge characteristics and nitrate retention by two Andepts from south-central Chile, *Soil. Sci. Soc. Am. Proc.*, 39, 842–846, 1975.

Gaudet, J. P., H. Jegat, G. Vachaud, and P. J. Wierenga, Solute transfer with exchange between mobile and stagnant water through unsaturated sand, *Soil Sci. Soc. Am. J.*, 41, 665–671, 1977.

Helfferich, F., *Ion Exchange*, McGraw-Hill, New York, 1962.

Hiester, N. K., and T. Vermeulen, Elution equations for adsorption and ion exchange in flow systems, *J. Chem. Phys.*, 16, 1087–1090, 1948.

Hiester, N. K., and T. Vermeulen, Saturation performance of ion exchange and adsorption columns, *Chem. Eng. Progr.*, 48, 505–516, 1952.

Hissink, D. J., Base exchange in soils, *Trans. Faraday Soc.*, 20, 551–566, 1924.

Hoffman, D. L., and D. E. Rolston, Transport of organic phosphate in soil as affected by soil type, *Soil Sci. Soc. Am. J.*, 44, 46–52, 1980.

Juda, W., and M. Carron, Equilibrium and velocity of sodium-hydrogen exchange on carbonaceous exchangers in contact with chloride solutions, *J. Am. Chem. Soc.*, 70, 3295–3300, 1948.

Lapidus, L., and N. R. Amundson, The rate-limiting steps in radial adsorption analysis, *J. Phys. Chem.*, 56, 373–383, 1952.

Lindstrom, F. T., R. Haque, V. H. Freed, and L. Boersma, Theory on the movement of some herbicides in soils, *Environ. Sci. Technol. 1*, 561–565, 1967.

Nkedi-Kizza, P., Ion exchange in aggregated porous media during miscible emplacement, Ph.D. dissertation, Dep. of Land, Air and Water Resour., Univ. of Calif., Davis, 1979.

Nkedi-Kizza, P., P. S. C. Rao, and J. M. Davidson, Ion-exchange and diffusive mass transfer during miscible displacement through an aggregated Oxisol, *Soil Sci. Soc. Am. J.*, 46, 471–476, 1982.

Nkedi-Kizza, P., J. W. Biggar, M. Th. van Genuchten, P. J. Wierenga, H. M. Selim, J. M. Davidson, and D. R. Nielsen, Modeling tritium and chloride 36 transport through an aggregated Oxisol, *Water Resour. Res.*, 19, 691–700, 1983.

Persaud, N., J. M. Davidson, and P. S. C. Rao, Miscible displacement of inorganic cations in a discrete homoionic exchange medium, *Soil Sci.*, 136, 269–278, 1983.

Rao, P. S. C., J. M. Davidson, R. E. Jessup, and H. M. Selium, Evaluation of conceptual models for describing nonequilibrium adsorption-desorption of pesticides during steady-state flow in soils, *Soil Sci. Soc. Am. J.*, 43, 22–28, 1979.

Rao, P. S. C., D. E. Rolston, R. E. Jessup, and J. M. Davidson, Solute transport in aggregated porous media: Theoretical and experimental evaluation, *Soil Sci. Soc. Am. J.*, 44, 1139–1146, 1980.

Selim, H. M., J. M. Davidson, and R. S. Mansell, Evaluation of a two-site adsorption-desorption model for describing solute transport in soil, Proceedings of the Computer Simulation Conference, Am. Inst. of Chem. Eng. Washington, D.C., pp. 444–448, 1976.

Singer, M. J., and P. Nkedi-Kizza, Properties and history of an exhumed tertiary Oxisol in California, *Soil Sci. Soc. Am. J.*, 44, 587–590, 1980.

Smith, J. M., Kinetics of adsorption, in *Adsorption From Aqueous Solutions, Adv. in Chem. Ser. 79*, pp. 8–22, American Chemical Society, Washington, D.C., 1968.

Thomas, H. C., Heterogeneous ion exchange in flowing systems, *J. Am. Chem. Soc.*, 66, 1664–1666, 1944.

van Genuchten, M. Th., Non-equilibrium transport parameters from miscible displacement experiments, *Res. Rep. 119*, U.S. Salinity Lab., Riverside, Calif., 1981.

van Genuchten, M. Th., and R. W. Cleary, Movement of solutes in soil: Computer-simulated and laboratory results, In *Soil Chemistry*, vol. B, *Physico-Chemical Models*, edited by G. H. Bolt, pp. 349–386, Elsevier, New York, 1979.

van Genuchten, M. Th., and P. J. Wierenga, Mass transfer studies in sorbing porous media, 1, Analytical solutions, *Soil Sci. Soc. Am. J.*, 40, 473–480, 1976.

van Raij, B., and M. Peech, Electrochemical properties of some oxisols and alfisols of the tropics, *Soil Sci. Soc. Am. Proc.*, 36, 587–593, 1972.

J. W. Biggar and D. R. Nielsen, Department of Land, Air and Water Resources, University of California, Davis, CA 95616.

J. M. Davidson and P. Nkedi-Kizza, Department of Soil Science, University of Florida, Gainesville, FL 32611.

H. M. Selim, Department of Agronomy, Louisiana State University, Baton Rouge, LA 70803.

M. Th. van Genuchten, U.S. Salinity Laboratory, U.S. Department of Agriculture, Riverside, CA 92501.

P. J. Wierenga, Department of Agronomy, New Mexico State University, Las Cruces, NM 88003.